Organic Chemistry Research

Article

Organic Chemistry Research
www.orgchemres.org

Cite this: *Org. Chem. Res.* **Year**, *Vol, 8*, 57-63.
DOI: 10.22036/org.chem.2023.414986.1296

Investigating of the Morphology of $MnMoO_4$ Nanocatalyst in Different Conditions and Its Effect on the Synthesis of γ-Amino Acids

Fatemeh Amarloo[a], Rahele Zhiani[a,b,*]

[a]*Department of Chemistry, Islamic Azad University, Neyshabur Branch, Neyshabur, Iran.*

[b]*New Materials Technology and Processing Research Center, Department of Chemistry, Neyshabur Branch, Islamic Azad University, Neyshabur, Iran. E-mail: r_zhiani2006@yahoo.com*

Received: October 12, 2023; Accepted: December 17, 2023

Abstract: The purpose of this study was to investigate the effect of different conditions on the microsphere morphology of $MnMoO_4$ nanofiber and the performance of $MnMoO_4$ nanocatalyst in the synthesis of γ-amino acids. The obtained results proved that, the effect of different mechanical pressures, time of hydrothermal processing and calcination on the amount of fibers and morphology of $MnMoO_4$ product is related. In addition, the reaction can be catalyzed through the photoredox catalyst and adapt to different amines and styrenes. Such a technique presents hugely functionalized γ-amino acids in adequate performances with utmost regioselection. The synthesis described here is the first instance of a γ-amino acid from CO_2 that has been visible-light-induced. The reaction in the presence of 20 mg of $MnMoO_4$ had a yield of 94%. Also, the reaction was not performed without light and catalyst. The catalyst was recycled 5 times and its performance was slightly reduced. It has many advantages, including no environmental damage, the least amount of catalyst due to its fiber structure, cost-effectiveness, operational simplicity, quick reaction times, high atom economy and perfect yields.

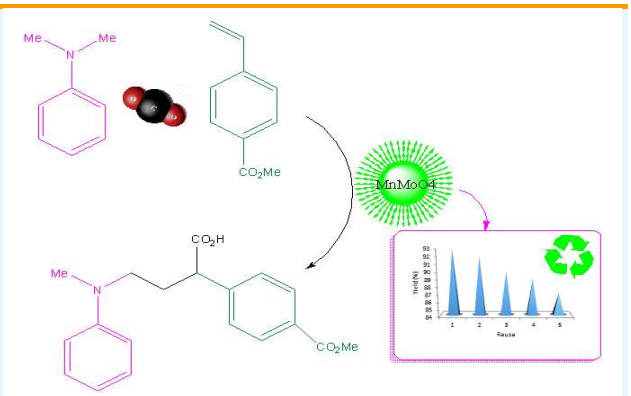

Keywords: γ-Amino acid, CO_2, Nanodendritic, $MnMoO_4$

1. Introduction

As a non-poisonous, ever-present, and recyclable carbon source, CO_2 has attracted considerable attention in the field of organic synthesis. The direct conversion of diluted CO_2 into favorable products, along with the suppression of other competing reactions has strategic importance while it is barely reported. Regarding the high thermodynamic stability of CO_2 linear molecule, the adsorption of CO_2 molecule onto the catalyst surface is signicance as non-linear CO_2 molecule on the catalysts is more destabilized compared to the linear one.[1–2] Zhang *et al*.[3] have shown the efficient photoreduction of diluted CO_2 through intruding -OH onto the Co-based MOFs and approving the key roles of high CO_2 binding affinity, which can ease the stability of the initial Co−CO_2 adduct and enhance the reduction of CO_2.

The catalytic carboxylation of non-saturated compounds with CO_2 has attracted the attention of chemists.[4] However; the photocatalytic functional carboxylation of alkenes with CO_2 is more demanding and barely reported. Recent research has shown, the photoredox-catalyzed the difunctionalization of alkenes in visible light to afford β-functionalized alkyl carboxylic acids with CO_2.[6]

In addition, γ-amino acids are highly strong composites and their global participation in pharmacy reflects their various biological usages. Furthermore, γ-amino acids deficiency is related to several significant neurological disorders like Huntington's and Parkinson's disease, epilepsy, and other psychiatric disorders, including anxiety and pain. [6, 7]

Based on the above-mentioned fact, the focus has been on the synthesis of γ-amino acids[8,9] similar to nitroethylene Michael addition of carbonyl compounds[10-12] or with unsaturated carbonyl compounds conjugate addition of nitroalkanes, in order to provide γ-amino acids.[13,14] Romero *et al.* have recently demonstrated the Y-amination of unsaturated acyl chlorides with azodicarboxylates, followed by the dihydropyridazinones' reductant ring for generating the amino acids.[15,16] These synthetic methods, however, have a limited bed range and difficult reaction conditions. Additionally, they require various steps to finish. The dicarbo-functionalization of alkenes and the synchronous amalgamation of carbon dioxide (CO_2) and aminoalkyl was proposed as the ideal method for transferring γ-amino acids. Chemists have paid close attention to organic

transformations brought on by visible light because of their demonstrated impact on organic synthesis expansion. Many photocatalyzed organic reactions such as unforeseen synthetic reactions were conducted via these synthetic platforms.[5] The Photoinitiated difunctionalization of carbon-carbon multiple bonds have been intensively used for producing structurally variable molecules.[16] The visible-light photo-redox catalysis is an empirical technique method for having access to open-shell radical species[17–19] and develops new approaches for the difunctionalization of alkenes.[20–22]

Photoredox-promoted single-electron oxidation of amines and following deprotonation to generate γ-aminoalkyl radicals have been explained.[23–26] It has been explained that photoredox-promoted single-electron oxidation of amines and subsequent deprotonation produce γ-aminoalkyl radicals. An alkyl radical species that underwent electron depletion in order to capture an electrophile[27– 30] was created as a result of the addition of γ-aminolemic radicals to alkenes.

It is anticipated that γ-amino acids may be produced as a result of CO_2 electrophile incorporation into the reaction compound. CO_2 has been found in organic synthesis as a non-poisonous, constantly present, and recyclable carbon source.[31– 33] Many chemists have been interested in the catalytic carboxylation of non-saturated compounds with CO_2 in comparison to the alkene hydrocarboxylation with it.[34– 37] Tian *et al*. synthesized nano $CuAl_2O_4$ in a new way. and used $CuAl_2O_4$ as a catalyst for the carbocarboxylation of styrenes based on CO_2 and amines.[38] Qin et al used CO_2 to synthesize γ-lactams.[39] Wang et al. reported the multicomponent carbonylation of γ-amino acids derivatives, which was obtained from the combination of amides, alkenes and carbon monoxide of γ-amino acids complex products.[41] Zhang et al. reported the synthesis of γ-amino acids by visible light carbocarboxylation of styrenes using CO_2 and amines by a photoredox catalyst.[42]

This eternal, general, and practical approach shows an unusual sample of redox-neutral dicarbofunctionalization of alkenes to create required γ-amino acids with utmost efficiency and selectivity in mild reaction situations. It provoked us to evaluate the microsphere formation potential of $MnMoO_4$ fibers using a controlled method and evaluate the effect of morphology regularly on the catalytic performance in the CO_2 stabilization reaction. Consistent with the present study on the synthesis and performance of heterogeneous catalysts in organic reactions, a simple programmable hydrothermal approach is presented here for the synthesis of nanocrystalline $MnMoO_4$ fiber anatomy of a spinel. It was investigated how various factors affected $MnMoO_4$ morphology and crystalline phase control. An aminomethylcarboxylation of alkenes with amines and CO_2 was used to assess the catalytic activity of synthesized fibrous MnMoO4 spheres. Additionally, this evolution has covered the relationships between these morphologies and how well they function as catalysts.

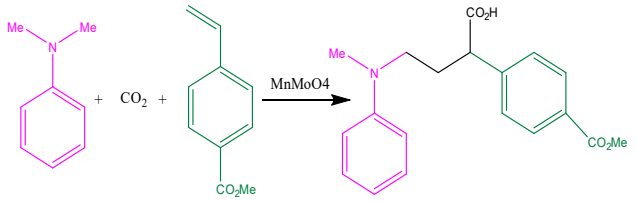

Scheme 1. γ-amino acid synthesis from CO_2 in the presence of $MnMoO_4$ NPs

2. Results and Discussion

Mesoporous and instance construction were determined using TEM and SEM. It is observed that the $MnMoO_4$ sample had a dandelion-like shape and the measure of the dandelions was consistent (Figure 1).

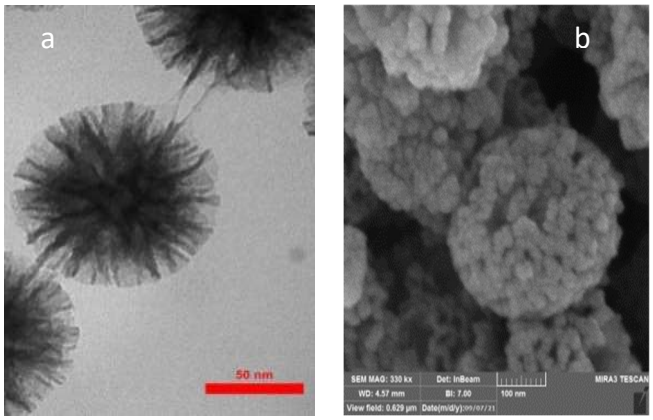

Figure 1. Images of filamentous $MnMoO_4$ (a) SEM, (b) TEM.

Evaluating these images confirmed that the substance has dendrimer fibers with a width of 20 nm acquired in three sizes to make the partitions. This could work with the great accessibility of the zone region. A progression of tests was performed to assess the impact of the quantity of CPB on the morphology of $MnMoO_4$. Without cetylpyridinium bromide only a modest quantity of $MnMoO_4$ was secluded and the nanostructures were monodispersed sans a filamentary construction (nanocomposite A, Figure 2a). This outcome confirmed the major duty of CPB in controlling the molecule measure and morphology of fibrous $MnMoO_4$. This impact was additionally seen when the various concentration of CPB was utilized to prepare fibrous $MnMoO_4$. TEM images indicated that fibrous $MnMoO_4$ started to develop from nanospheres (nanocomposite B, Figure 2b). At first, fibers were so unable (nanocomposite C, Figure 2c) and finally consolidated (nanocomposite D, Figure 2d) when the quantity of CPB develops from 0.5 g upper to 1.5 g.

Subsequent to analyzing the mechanical stability of $MnMoO_4$ NPs as fibers, NPs were examined by using the SEM analysis. The string construction of $MnMoO_4$ NP fibers stayed without changing downward mechanical pressure upper to 150 bar (Figure 3a-b).

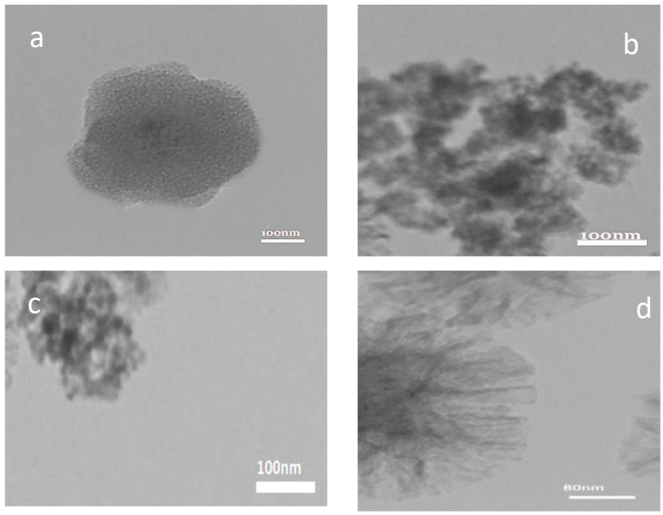

Figure 2. TEM photos of fibrous $MnMoO_4$ nanostructures with (a) 0.0 g, (b) 0.5 g, (c) 0.1 g, and (d) 1.5 g of CPB per 1.3 mL of aqueous 45 mM of $Mn(NO_3)_2.6H_2O$ or $Na_2MoO_4 \cdot 2H_2O$.

Fibrous $MnMoO_4$ NPs formation uncovered the great mechanical resistors that could be credited to their attendance of narrow filaments and high porosity by a fence - like an anatomy. Additionally, as shown in Figure 3c fibrous $MnMoO_4$ NPs had excellent thermic resolvent consistency and unchanged structures after a thermal treatment in hot dimethyl sulfoxide (DMSO) for 72 h.

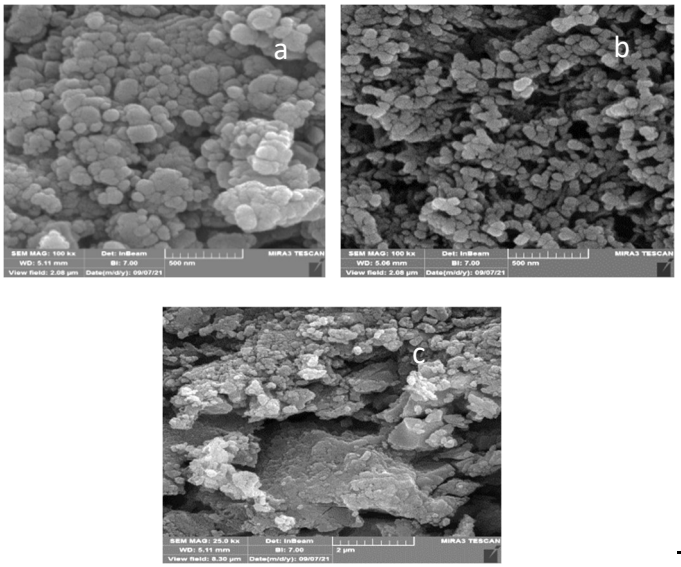

Figure 3. SEM images of mechanical stability of $MnMoO_4$ nanoparticles at pressures a) 75 MPa, b) 150 MPa, c) after heating in DMSO solution for 3 days.

The thermal stability of $MnMoO_4$ nanoparticles was investigated at temperatures from 300 to 800°C. According to the SEM analysis of these nanoparticles, which you can see in Figure 4, the morphology and size of the nanoparticles did not change significantly and they were resistant to heat.

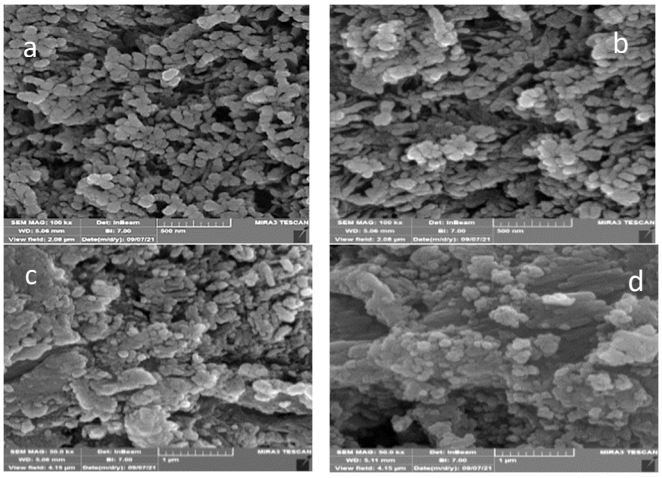

Figure 4. SEM images after calcination at 300 °C/3 h (a), 400 °C/3 h (b), 600 °C/3 h (c), and up to 800 °C/3 h (d).

This perusal indicated that there was not any coagulation after serious heat treatment. This data is significant since heat resistor is a critical situation for catalysts which are dynamic in excessive exothermal areas. Absorption - desorption isotherms of N_2 from the sinewy $MnMoO_4$ nanostructure indicate the attributes of the kind IV curvature (Figure 5).

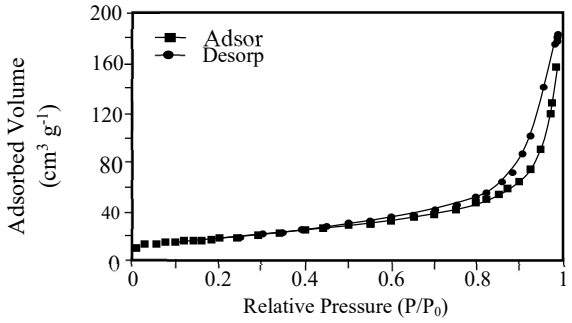

Figure 5. The N_2 adsorption–desorption isotherms of fibrous $MnMoO_4$ NPs.

BJH hole diameter, BET outside substrate, and whole pore volume were 158 $m^2. g^{-1}$ and 1.19 $cm^3. g^{-1}$, 8.78 nm, individually. Based on the Table 1, these results can confirm the fibrous construction of the catalyst.

Table 1. Fibrous anatomical factors of $MnMoO_4$ NP material take from nitrogen absorption tests

Catalysts	S_{BET} (m^2g^{-1})	V_T(cm^3g^{-1})	D_{BJH} (nm)
Fibrous $MnMoO_4$ NPs	158	1.19	8.78

The catalyst was introduced at different light powers (8, 15, 20, 22, and 32 W) with other consistent items to accomplish yield of 12, 25, 90, 91, and 94%. The production of γ-amino acids bit by bit upgraded with light power ranged from 8-20 watts and stayed steady at 20 watts. However, the utilization

of higher CFL watts (22 W) had no critical impact on the efficiency or response time.

The amount of the catalyst assumed a fundamental part in the carbocarboxylation of styrene utilizing CO_2 and amines because the response doesn't go on without even a trace of the catalyst. The generation of γ-amino acids was started in the participation of at least 5 mg of $MnMoO_4$ as a catalyst in great response condition with an efficiency of 16% (Figure 6).

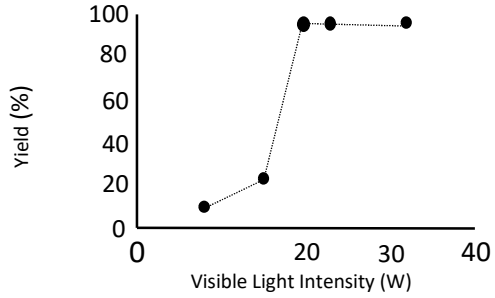

Figure 6. lamp Infiltrations on the response method.

Improving the quantity of catalyst did not develop the item production (Figure 7). In addition, a progression of inductive tests was performed. The lack of γ-amino acids downward dark condition demonstrated the photocatalytic origin of the response. Without $MnMoO_4$ NPs or TEOA, γ-amino acids were not produced under visual light radiance. To examine the origin of the created γ-amino acids, N_2 (rather than CO_2) was utilized to preprocess of $MnMoO_4$ NPs and the dissolvable group. Under radiance and following 30 min, just a hint of γ-amino acids was gotten in the group of $MnMoO_4$ NPs as the photo catalyst.

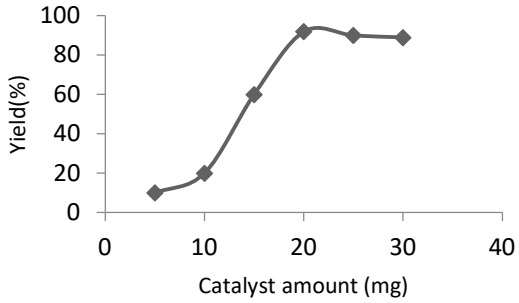

Figure 7. The result of catalyst content.

It was demonstrated that the γ-amino acids were obtained from CO_2 rather than the deterioration of ligands (Figure 8). To survey the specific effect of the attendance of fiber microspheres in the construction of $MnMoO_4$, the fibrous $MnMoO_4$ (Nano composition D) was evaluated with other nanocomposites A, B, and C (Figure 2). When nanocomposites A, B, and C were utilized as catalysts, the efficiency of the output was mild to excellent; but, the efficiency was great for fibrous $MnMoO_4$ (Nano composition D). The Unavoidable movement of the $MnMoO_4$ was determined to be due to its synthesis, form, and morphology. In addition, the enormous area among the fibers can fundamentally growth the availability of $MnMoO_4$ active sites.

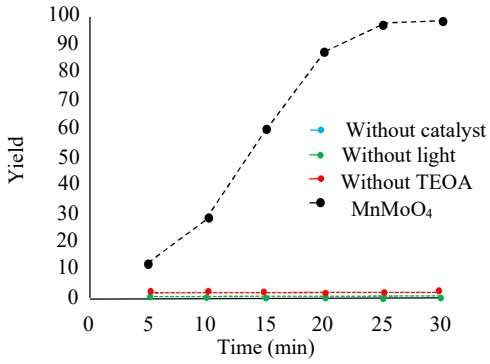

Figure 8. The amount of Y-amino acids produced as a function of irradiation time under different conditions.

It proved that fibrous $MnMoO_4$ (nano composition D) was more efficient compared to nanocomposites A, B, and C (Table 2). The renewability of a catalyst was viewed as a vital representative in green chemistry. Thusly, the reusability of $MnMoO_4$ NPs was ideally inspected for the carbocarboxylation of styrene utilizing CO_2 and amines. After the response was finished, the solid $MnMoO_4$ NPs were quickly eliminated from the fluid response area within a couple of moments. The solver could be reutilized quickly in the wake of cleaning.

Table 2. Effect of various catalysts on the γ-amino acids synthesis

Entry	Catalyst	Yield (%)
1	Nanocomposition A	18
2	Nanocomposition B	38
3	Nanocomposition C	69
4	Nanocomposition D	94

As shown in Figure 9, the catalyst was reutilized following 5 continuous stages. The output efficiency in the 5th run was 87%, demonstrating a 7% reduction in the efficiency in comparison with the new catalysts (94%). Besides, thorough research was done on the heterogeneity of the catalysts. In the first step, a hot purification test was accomplished to create γ-amino acids under higher-level circumstances and the catalyst was taken out after 3 hours at an efficiency of 39%. After the evacuation of the heterogeneous catalysts, it was observed that the gratis catalysts deposits were generally dynamic, and following 9 hours of cyclic carbonate generation, 69% change was accomplished. This indicated that the catalysts worked heterogeneously within the response and halfway filtering occurred in the response. Afterward, a mercury-toxication experiment was accomplished to ensure the catalyst's heterogeneity. In

addition, it strikingly nullified the metal catalysts on the dynamic layer, and in this way, down warded the catalyst's action. The experimental outcomes affirmed the catalyst's heterogeneity. This experiment was accomplished on the ideal response mode under an ideal condition.

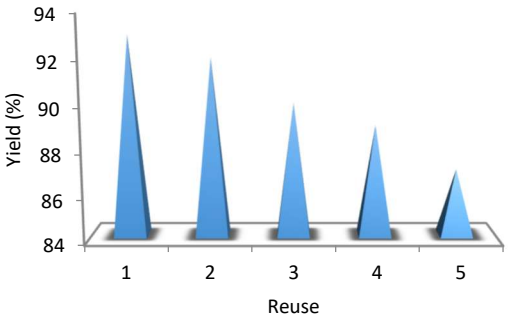

Figure 9. Catalyst recyclability.

Around 300 molar mercury was distributed to the response synthesis following 5 hours and blended. There were not any changes during the 10 hours. Figure 10 portrays the kinetics plan of the response in the participation of Hg (0). Adverse outcome of the heterogeneity tests (hot purification and Hg (0) toxication) exhibit that the hard catalysts are heterogeneous and there is not any metal filtering in the generation of cyclic carbonate.

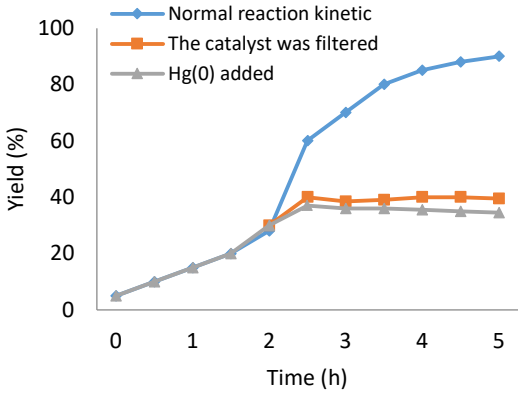

Figure 10. Response kinetics, Hg (0) toxication, and hot purification studies for the synthesis of γ-amino acids.

The TEM images gave more data about fibrous $MnMoO_4$ NPs. Figure 11 the five-time reused fibrous $MnMoO_4$ NPs. After five repetitions, the wall-like catalyst structure was yet visual. The similarity of the fibrous construction of new $MnMoO_4$ NPs and five -time reused $MnMoO_4$ NPs showed a high strength for catalyst recyclability.

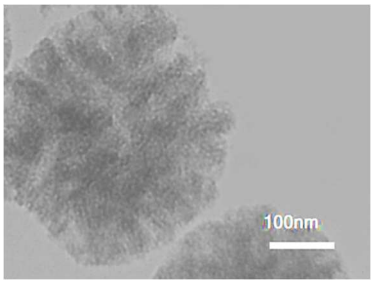

Figure 11. TEM image of fibrous $MnMoO_4$ NPs after five reuses.

The thermal stability of the fresh catalyst after five times was compared with the recycled catalyst. The thermal stability of the recycled catalyst did not change up to 100 °C, but decreased at higher temperatures. This may be due to the loss of the catalyst surface during recycling (Figure 12).

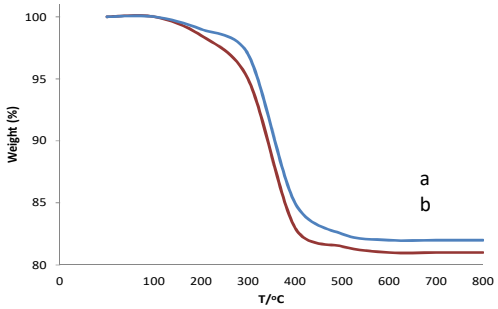

Figure 12. TGA (a) fresh catalyst, (b) recycled catalyst after five reuses

Based on the above results, a plausible mechanism was proposed and shown in Scheme 2. In compound 1, aniline is excited by $MnMoO_4$ and is converted into an intermediate radical cation (intermediate A) and protonated and produces α-aminoalkyl radical B. The electron of carbon radical B attacks the C=C bond of compound 2. to selectively generate γ-amino C benzyl radical. Nucleophilic addition to CO_2 and protonation completes the reaction, producing the expected γ-amino acids.

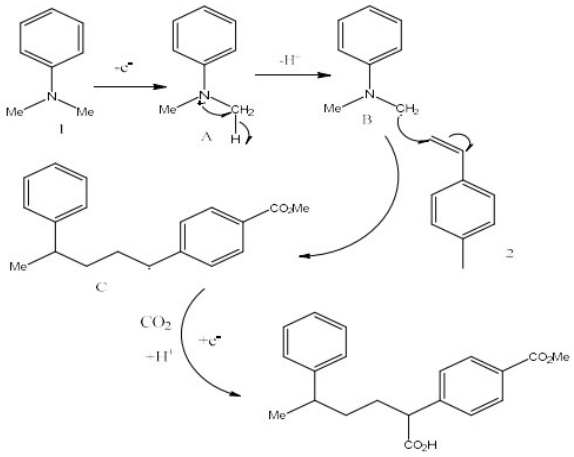

Scheme 2. Mechanism of γ-amino acid synthesis

3. Experimental

The global method for fabricating fibrous $MnMoO_4$ NPs

The following amounts of substances were solved in 1-pentanol (0.020 L) and cyclohexane (500 ml) solution: 1.2 ml of water, 5 ml of $Na_2MoO_4{\cdot}2H_2O$, and 2.2 ml of $Mn(NO_3)_2.6H_2O$. The released solution was a combination of cetylpyridinium bromide (1.2 g) and 2ml of 0.05 M ascorbic acid combined for 45 minutes at 25 °C. The combination was then heated for 6 hours at 110 °C in a Teflon-sealed hydrothermal reactor. A centrifuge was used to extract $MnMoO_4$ filamentous NPs, followed by washing with acetone and deionized water before drying in oven. To remove unreacted metal salts and ligands from the freshly formed $MnMoO_4$, photocatalytic processes were washed with DMF. The sample was then placed in acetonitrile for 10 hours to saturate and replace the solvent. Then the item was dissipated and refined utilizing carbon dioxide. $MnMoO_4$ (20.0 mg) was delivered into a CH_3CN/TEOA blend (50 mL, V/V = 1.25), which had effectively been gassed with CO_2 for 6 h. Photocatalytic responses, except for the N_2 control explore, acted in an environment of carbon dioxide at surrounding pressure. The response was lighted with a 22 watts fluorescent light (CFL). The light was 10 cm away from the response bottle. $MnMoO_4$ (25 mg) was delivered to a 20 mL Schlenk tube by a piece magnetic stir bar. The cylinder was purged and occupied with CO_2 multiple times. Anhydrous DMSO (1 mL), methyl 4-vinyl benzoate (16 mg), and N, N-dimethylaniline (75 mg) were delivered in a cylinder under CO_2 positive environment. The response tube was tightly closed and blended at room temperature and under a 22 watt fluorescent light (CFL) for 24 hours. Then, the response was thoroughly extinguished with 2 M HCl, and the mix was taken out by ethyl acetic acid derivation (30 mL). The composite natural layers were dried over anhydrous Na_2SO_4 and concentrated under diminished pressure. Ether: After that $TMSCHN_2$ (200 mL, 2 M in hexane) and MeOH (2: 2) (1.0 mL) were then delivered to the response combination and mixed at 0 ℃ for 40 minutes. After, the yields were indicated by the GC strategy utilizing n-dodecane (25 mL) as an inner norm in the following esterification.

Generated $MnMoO_4$ filamentary nanoparticles carried out by microemulsion using dysprosium nitrate and Ceric Ammonium Nitrate (CAN). Furthermore, cetyl pyridinium bromide (CPB) was used as a mold in a mixture of cyclohexane, water, and pentanol. $MnMoO_4$ was considered as unrefined components that consumed the accessible gratis area in the mold.

After progressive centrifugation/ washing by suitable dissolvable, the efficiency was great at this point.

γ-Amino acid synthesis

$MnMoO_4$ (20 mg) was released into a Schlenk tube with a magnetic stir bar. The tube was emptied and filled with CO_2 thrice. Then, anhydrous DMSO (1 ml), methyl 4-vinylbenzoate (15 mg), and *N*,*N*-dimethyl aniline (70 mg) were released into the tube under a positive CO_2 environment. The reaction tube was sealed and mixed at r.t. under a 22 W compact fluorescent lamp (CFL) for 24 h. When the reaction was over, it was watchfully extinguished with HCl (2 M). The blend was drawn out with EtOAc (4 5 ml). The composite organic layers were dried over anhydrous Na_2SO_4. Then, ether: methanol (1: 1) (1.0 ml) and $TMSCHN_2$ (200 ml, 1 M in hexane) were released into the reaction blend and stirred at 0 ºC for 30 min.

2-(4-(Methoxycarbonyl)phenyl)-4-(methyl(phenyl)amino) butanoic acid: ^{13}C NMR ($CDCl_3$, 600 MHz) d 178.52, 166.89, 149.12, 143.22, 130.31, 129.69, 129.41, 128.31, 117.09, 112.89, 52.29, 50.88, 49.33, 38.82, 30.01. ^{1} H NMR ($CDCl_3$, 600 MHz) d 8.01 (d, J ¼ 8.0 Hz, 2H), 7.41 (d, J ¼ 7.9 Hz, 2H), 7.19 (t, J ¼ 7.8 Hz, 2H), 6.71 (t, J ¼ 7.2 Hz, 1H), 6.59 (d, J ¼ 8.1 Hz, 2H), 3.89 (s, 3H), 3.71 (s, 1H), 3.37 (m, 1H), 3.32–3.21 (m, 1H), 2.79 (s, 3H), 2.40 (m, 1H), 2.21–1.89 (m, 1H).

4. Conclusions

A new group of $MnMoO_4$ NPs with an exceptional fibrous $MnMoO_4$ morphology was introduced. Fibrous $MnMoO_4$ NPs give away magnificent attributes same as the several vigorous dynamic sites, high thermal and mechanical resistors, and excessive outside substrate. It can be a utilitarian catalyst for different responses because of its magnificent characteristics. Extensive outside space, because of the presence of relevant grooves and dendrimer wall-like filament NPs, filamentary $MnMoO_4$ nanoparticles can be utilized in different scientific applications. $MnMoO_4$ has astounding catalytic effectiveness and acts as a desirable heterogeneous group for the chemical consolidation of CO_2 in amines and alkenes. Sans decreasing action and compound, the catalysts can be reutilized in around five runs.

Declaration of Interests

The authors declare that they have no known competing financial interests or personal relationships that could have appeared to influence the work reported in this paper.

Author Contributions

Fatemeh Amarloo: Investigation, Methodology, Data curation, Writing-Original draft preparation. Rahele Zhiani: Supervision, Conceptualization, Writing-Reviewing and Editing, Visualization, Validation.

Author(s) ID

Fatemeh Amarloo: 0009-0009-5397-4523
Rahele Zhiani: 0000-0002-2051-0054

References

1. W. Tu, Y. Zhou, Z. Zou, *Adv. Mater.*, **2014**, *26*, 4607-4626.
2. X. Chang, T. Wang, J. Gong, *Energy Environ. Sci.* **2016**, *9*, 2177-2196.
3. M. Zhou, S. Wang, P. Yang, C. Huang, X. Wang, *ACS Catal.* **2018**, *8*, 4928-4936.
4. N. A. Romero, D. A. Nicewicz, *Chem. Rev.* **2016**, 116, 10075-10166.
5. K. M. Nakafuku, S. C. Fosu, D. A. Nagib, *J. Am. Chem. Soc.* **2018**, *140*, 11202-11205.
6. Y. Wang, N. Y. Huang, J. Q. Shen, P. Q. Liao, X. M. Chen, J. P. Zhang, *J. Am. Chem. Soc*. **2018**, *140*, 38-41.
7. P. Conti, L. Tamborini, A. Pinto, A. Blondel, P. Minoprio, A.

Mozzarelli, C. De Micheli, *Chem. Rev.* **2011**, *111*, 6919-6946.
8. R. B. Silverman, Angew. *Chem. Int. Ed*. **2008**, *47*, 3500-3504.
9 . M. Ordóñez, C. Cativiela, *Tetrahedron Asymmetry,* **2007**, *18*, 3-99.
10. K. Maruoka, Takashi Ooi, *Chem. Rev*. **2003**, *103*, 3013-3028.
11. R. Kastl, H. Wennemers, *Angew. Chem*. **2013**, *125*, 7369-7373.
12. J. H. Sim, C. E. Song, *Angew. Chem*. **2017**, *129*, 1861-1865.
13. Y. Chi, L. Guo, N. A. Kopf, S. H. Gellman*, J. Am. Chem. Soc.* **2008**, *130*, 5608-5609.
14. K. Akagawa, K. Kudo, *Angew. Chem*. **2012**, *124*, 12958-12961.
15. A. Baschieri, L. Bernardi, A. Ricci, S. Suresh, M. F. A. Adamo, *Angew. Chem.* **2009**, *121*, 9506-9509.
16. X. Y. Chen, F. Xia, J. T. Cheng, S. Ye, Angew. *Chem. Int. Ed.,* **2013**, *52*, 10644-10647.
17. B. Zhang, Y. Yi, Z. Q. Wu, C. Chen, C. Xi, *Green Chem*. **2020**, *22*, 5961-5965.
18. D. Ravelli, S. Protti, M. Fagnoni, *Chem. Rev*., **2016**, *116*, 9850-9913.
19. D. H. Kim, S. I. Woo, J. M. Lee, O. B. Yang*, Catal. Lett*., **2000**, *70*, 35-41.
20. J. P. Goddard, C. Ollivier, L. Fensterbank, *Acc. Chem. Res*., **2016**, *49*, 1924-1936.
21. M. Y. Cao, X. Ren, Z. Lu, *Tetrahedron Lett*., **2015**, *56*, 3732-3742.
22. T. Koike, M. Akita, *Org. Chem. Front*. **2016**, *3*, 1345-1349.
23. T. Koike, M. Akita, *Chem*., **2018**, *4*, 409-437.
24. M. H. Shaw, V. W. Shurtleff, J. A. Terrett, J. D. Cuthbertson, D. W. C. *MacMillan, Science.,* **2016**, *352*, 1304-1308.
25. S. M. Saadati, S. M. Sadeghzadeh, *Catal. Lett*., **2018**, *148*, 1692-1702.
26. L. Shi, W. Xia, *Chem. Soc. Rev*., **2012**, *41*, 7687-7697.
27. S. A. Morris, J. Wang, N. Zheng, *Acc. Chem. Res*., **2016**, *49*, 1957-1968.
28. Y. Miyake, K. Nakajima, Y. Nishibayashi, *J. Am. Chem. Soc*. **2012**, *134*, 3338-3341.
29. P. Kohls, D. Jadhav, G. Pandey, O. *Reiser, Org. Lett*., **2012**, *14*, 672-675.
30. Y. Yin, Y. Dai, H. Jia, J. Li, L. Bu, B. Qiao, X. Zhao, Z. Jiang, *J. Am. Chem. Soc*., **2018**, *140*, 6083-6087.
31. M. A. Ashley, C. Yamauchi, J. C. K. Chu, S. Otsuka, H. Yorimitsu, T. Rovis, *Angew. Chem. Int. Ed*., **2019**, *58*, 4002-4006.
32. D. Yu, S. P. Teong, Y. Zhang, *Coord. Chem. Rev*., **2015**, *293*, 279-291.
33. Y. Tsuji, T. Fujihara, *Chem. Comm*., **2012**, *48*, 9956-9964.
34. S. Wang, C. Xi, *Chem. Soc. Rev*., **2019**, *48*, 382-404.
35. A. Tortajada, F. Juliá-Hernández, M. Börjesson, T. Moragas, R. Martin, *Angew. Chem. Int. Ed*. **2018**, *57*, 15948-15982.
36. S. M. Sadeghzadeh, R. Zhiani, M. Moradi, *ChemistrySelect* , **2018**, *3*, 3516-3522.
37. F. Juliá-Hernández, M. Gaydou, E. Serrano, M. van Gemmeren, R. Martin, *Ni-and Fe-Based Cross-Coupling Reactions,* **2017**, 91-128.
38. S. Tian, Q. Yang, S. M. Sadeghzadeh, *New J. Chem*. **2021**, *45*, 8942-8948.
39. Qin, R. Cauwenbergh, S. Pradhan, R. Maiti, P. Franck, S. Das, *Nature Communications*, **2023**, *14* , 7604.
40. L. C. Wang, Y. Yuan, Y. Zhang, X. F. Wu, *Nature Communications*, **2023**, *14*, 7439.
41. B. Zhang, Y. Yi, Z. Q. Wu, C. Chen, C. Xi, *Green Chem*., **2020**, *22*, 5961-5965.